VOLUME 122, NUMBER 14
APRIL 12, 2000

JOURNAL OF THE AMERICAN CHEMICAL SOCIETY

Crystal Structure of the Ribonucleotide Reductase R2 Mutant that Accumulates a μ-1,2-Peroxodiiron(III) Intermediate during Oxygen Activation

Walter C. Voegtli,[†] Nelly Khidekel,[†] Jeffrey Baldwin,[‡] Brenda A. Ley,[‡] J. Martin Bollinger, Jr.,*[,‡] and Amy C. Rosenzweig*[,†]

Contribution from the Departments of Biochemistry, Molecular Biology, and Cell Biology and of Chemistry, Northwestern University, Evanston, Illinois 60208, and the Department of Biochemistry and Molecular Biology, The Pennsylvania State University, University Park, Pennsylvania 16802

Received June 2, 1999. Revised Manuscript Received January 17, 2000

Abstract: The R2 subunit of *Escherichia coli* (aerobic) ribonucleotide reductase activates molecular oxygen at its diiron center to produce a functionally essential stable tyrosyl radical from residue Y122. It was previously shown that the D84E site-directed mutant of R2 (R2-D84E) accumulates a μ-1,2-peroxodiiron(III) intermediate on the pathway to tyrosyl radical formation. This intermediate does not accumulate in the reaction of wildtype (wt) R2, but an analogous complex does accumulate during oxygen activation by the structurally similar diiron protein, methane monooxygenase hydroxylase (MMOH). Herein we describe the crystallographically determined three-dimensional structures of the reduced, diiron(II) reactant and oxidized, diiron(III) product forms of R2-D84E. The reduced R2-D84E structure differs from that of reduced wt R2 in the conformations of three carboxylate ligands, E84, E204, and E238. The adjustments in these ligands render the coordination sphere of the diiron(II) center very similar to that in reduced MMOH. In addition, a water molecule not observed in reduced wt R2 is coordinated to Fe2 in reduced R2-D84E. The oxidized R2-D84E structure is similar to that of oxidized wt R2 except in the coordination mode of E84. In R2-D84E, E84 coordinates to Fe1 in a monodentate, terminal mode and is hydrogen bonded to a water molecule also coordinated to Fe1. In wt R2, D84 is a bidentate, chelating ligand. In both R2-D84E structures, Y122 is shifted away from Fe1 such that a hydrogen bonding interaction with E84 is not possible. The observed structural adjustments suggest possible rationales for the stability of the μ-1,2-peroxodiiron(III) complex in R2-D84E. In addition, the structures expand the experimental foundation for computational investigations aimed at defining the detailed mechanistic pathways for O_2 activation at diiron(II) centers.

Introduction

The R2 subunit of ribonucleotide reductase,[1] the hydroxylase component of methane monooxygenase (MMOH), and stearoyl acyl carrier protein Δ-9 desaturase (Δ9D) are the most extensively studied members of a family of proteins that utilize carboxylate-bridged diiron(II) clusters to activate O_2 for difficult oxidation reactions. Despite having similar tertiary structures and diiron active centers,[2] these proteins mediate chemically distinct reactions. In R2, O_2 is activated stoichiometrically to produce a functionally essential tyrosyl radical by the one-electron oxidation of a tyrosine residue.[3] In MMOH and Δ9D,

* To whom correspondence should be addressed.
[†] Northwestern University.
[‡] The Pennsylvania State University.

10.1021/ja991839l CCC: $19.00
Published on Web 03/28/2000

catalytic O_2 activation results in the hydroxylation of methane and the dehydrogenation of an acyl group, respectively, which are both two-electron oxidations.[4] The structural bases for the divergent control of O_2 activation by these related proteins have not yet been defined.

Previous kinetic and spectroscopic studies on the R2 and MMOH reactions revealed a key mechanistic difference that correlates with their divergent outcomes. The MMOH reaction proceeds sequentially through two intermediates, **P** (or $\mathbf{H_{peroxo}}$) and **Q**, of which each is two electrons more oxidized than the product diiron(III) cluster. Intermediate **P**, which is probably a μ-1,2-peroxodiiron(III) complex, forms first[5−7] and is converted without net reduction to the (formally) diiron(IV) complex **Q**, which is implicated as the species that hydroxylates methane.[6,8−10] By contrast, in the reaction of R2 from *E. coli*, neither a peroxodiiron(III) nor a diiron(IV) complex accumulates to a high level, and consequently, neither has been conclusively demonstrated as an intermediate. Instead, the rapid injection of an "extra" electron (which can be provided by excess Fe^{2+} or ascorbate, if either is present) upon reaction of the diiron(II) cluster with O_2 results in accumulation of a stoichiometric quantity of the formally Fe(III),Fe(IV) cluster **X**.[11−15] Conversion of **X** to the product μ-oxodiiron(III) cluster is accompanied by one-electron oxidation of Tyr122 to the radical.[16]

Although existing evidence for the intermediacy of a **P**-like peroxodiiron(III) complex in the R2 reaction is inconclusive,[12] nearly all recent mechanistic proposals have invoked such a species.[17−22] A recent kinetic study has provided evidence that, if a **P** cognate does form on the pathway to cluster **X**, then it must decay with a rate constant exceeding 400 s^{-1} at 5 °C.[23,24] This is much greater than the 0.5−1.2 s^{-1} (at 4 °C) with which **P** itself is converted to **Q** in MMOH.[6,7,25] Moreover, the μ-1,2-peroxodiiron(III) complex formed during the unproductive oxidation of chemically reduced Δ9D decays remarkably slowly, with a rate constant of 7×10^{-5} s^{-1} at 6 °C.[26] Thus, if a **P** cognate is also involved in the R2 reaction, the three proteins must differentially modulate the lifetime of the common peroxodiiron(III) unit by more than a million-fold. Alternatively, a structurally distinct adduct may form in the R2 reaction. This adduct might have a greater inherent reactivity toward one-electron reduction than the μ-1,2-peroxodiiron(III) complex, a difference that might be important in distinguishing the R2 mechanistic pathway from those of MMOH and Δ9D. Either scenario, modulation of the reactivity of a common peroxodiiron(III) adduct or formation of structurally distinct adducts, is likely to reflect functionally significant "tuning" of the reactivity of the diiron center as a result of differences in cluster coordination and active site structure among the proteins.

Consistent with this notion, we recently showed that a relatively long-lived ($t_{1/2}$ of 1 s at 5 °C) μ-1,2-peroxodiiron(III) intermediate having optical and Mössbauer spectroscopic features in common with MMOH **P** and the peroxo adduct in Δ9D accumulates on the reaction pathway leading to the tyrosyl radical in a variant of R2 in which the amino acid iron ligands have been rendered identical with those in MMOH and Δ9D by substitution of Fe1 ligand Asp84 with Glu.[22,33] To uncover the structural basis for the effect of this apparently conservative substitution, we have now characterized the reactant diiron(II) and product diiron(III) forms of R2-D84E by X-ray crystallography. In the former structure, several striking adjustments in coordination render its diiron(II) cluster more similar to that in reduced MMOH than to that in reduced wt R2. This correlation suggests that the specific coordination geometry in MMOH and R2-D84E is particularly suited to formation or stabilization of the μ-1,2-peroxodiiron(III) adduct. In addition,

(1) Abbreviations used: R2, R2 subunit of ribonucleotide reductase; MMOH, hydroxylase component of methane monooxygenase; R2-D84E, D84E mutant of the R2 subunit of ribonucleotide reductase; wt R2, wild-type R2 subunit of ribonucleotide reductase; Δ9D, stearoyl acyl carrier protein Δ-9 desaturase; EMTS, sodium ethylmercurithiosalicylate; CD/MCD, circular dichroism and magnetic circular dichroism spectroscopy.

(2) Nordlund, P.; Eklund, H. *Curr. Op. Struct. Biol.* **1995**, *5*, 758−766.
(3) Sjöberg, B.-M. *Struct. Bonding* **1997**, *88*, 139−173.
(4) Wallar, B. J.; Lipscomb, J. D. *Chem. Rev.* **1996**, *96*, 2625−2657.
(5) Liu, K. E.; Wang, D.; Huynh, B. H.; Edmondson, D. E.; Salifoglou, A.; Lippard, S. J. *J. Am. Chem. Soc.* **1994**, *116*, 7465−7466.
(6) Liu, K. E.; Valentine, A. M.; Wang, D.; Huynh, B. H.; Edmondson, D. E.; Salifoglou, A.; Lippard, S. J. *J. Am. Chem. Soc.* **1995**, *117*, 10174−10185.
(7) Valentine, A. M.; Stahl, S. S.; Lippard, S. J. *J. Am. Chem. Soc.* **1999**, *121*, 3876−3887.
(8) Lee, S.-K.; Fox, B. G.; Froland, W. A.; Lipscomb, J. D.; Münck, E. *J. Am. Chem. Soc.* **1993**, *115*, 6450−6451.
(9) Lee, S.-K.; Nesheim, J. C.; Lipscomb, J. D. *J. Biol. Chem.* **1993**, *268*, 21569−21577.
(10) Shu, L.; Nesheim, J. C.; Kauffmann, K.; Münck, E.; Lipscomb, J. D.; Que, L., Jr. *Science* **1997**, *275*, 515−518.
(11) Bollinger, J. M., Jr.; Edmondson, D. E.; Huynh, H.; Filley, J.; Norton, J. R.; Stubbe, J. *Science* **1991**, *253*, 292−298.
(12) Tong, W. H.; Chen, S.; Lloyd, S. G.; Edmondson, D. E.; Huynh, B. H.; Stubbe, J. *J. Am. Chem. Soc.* **1996**, *118*, 2107−2108.
(13) Sturgeon, B. E.; Burdi, D.; Chen, S.; Huynh, B.-H.; Edmondson, D. E.; Stubbe, J.; Hoffman, B. H. *J. Am. Chem. Soc.* **1996**, *118*, 7551−7557.
(14) Willems, J. P.; Lee, H.-I.; Burdi, D.; Doan, P. E.; Stubbe, J.; Hoffman, B. M. *J. Am. Chem. Soc.* **1997**, *119*, 9816−9824.
(15) Riggs-Gelasco, P. J.; Shu, L.; Chen, S.; Burdi, D.; Huynh, B. H.; Que, L., Jr.; Stubbe, J. *J. Am. Chem. Soc.* **1998**, *120*, 849−860.
(16) Bollinger, J. M., Jr.; Tong, W. H.; Ravi, N.; Huynh, B. H.; Edmondson, D. E.; Stubbe, J. *J. Am. Chem. Soc.* **1994**, *116*, 8015−8023.
(17) Andersson, M. E.; Högbom, M.; Rinaldo-Matthis, A.; Andersson, K. K.; Sjöberg, B.-M.; Nordlund, P. *J. Am. Chem. Soc.* **1999**, *121*, 2346−2352.
(18) Lange, S. J.; Que, L., Jr. *Curr. Op. Chem. Biol.* **1998**, *2*, 159−172.
(19) Stubbe, J.; Riggs-Gelasco, P. *Trends Biochem. Sci.* **1998**, *23*, 438−443.
(20) Eklund, H.; Eriksson, M.; Uhlin, U.; Nordlund, P.; Logan, D. *Biol. Chem.* **1997**, *378*, 821−825.
(21) Huynh, B. H.; Bollinger, J. M., Jr.; Edmondson, D. E. In *Spectroscopic Methods in Bioinorganic Chemistry*; ACS Symp. Ser. No. 692; Solomon, E. I., Hodgson, K. O., Eds.; American Chemical Society: Washington, DC, 1998; pp 403−422.
(22) Moënne-Loccoz, P.; Baldwin, J.; Ley, B. A.; Loehr, T. M.; Bollinger, J. M., Jr. *Biochemistry* **1998**, *37*, 14659−14663.
(23) Baldwin, J.; Krebs, C.; Ley, B. A.; Edmondson, D. E.; Huynh, B. H.; Bollinger, J. M., Jr. Manuscript in preparation.
(24) Formation of a transient tryptophan cation radical, a species that would necessarily be preceded in the mechanistic sequence by the presumptive peroxodiiron(III) intermediate, was demonstrated to be kinetically first order in both reactants (O_2 and Fe(II)−R2 complex). This observation implies that very little of an intermediate preceding the tryptophan cation radical can accumulate. Kinetic simulations suggested a lower limit for decay of an intervening species (such as the peroxodiiron(III) species) of ∼400 s^{-1}.
(25) Nesheim, J. C.; Lipscomb, J. D. *Biochemistry* **1996**, *35*, 10240−10247.
(26) Broadwater, J.; Achim, C.; Munck, E.; Fox, B. G. *Biochemistry* **1999**, *38*, 12197−12204.
(27) Nordlund, P.; Sjöberg, B.-M.; Eklund, H. *Nature* **1990**, *345*, 593−598.
(28) Logan, D. T.; Su, X.-D.; Åberg, A.; Regnström, K.; Hajdu, J.; Eklund, H.; Nordlund, P. *Structure* **1996**, *4*, 1053−1064.
(29) Rosenzweig, A. C.; Frederick, C. A.; Lippard, S. J.; Nordlund, P. *Nature* **1993**, *366*, 537−543.
(30) Rosenzweig, A. C.; Nordlund, P.; Takahara, P. M.; Frederick, C. A.; Lippard, S. J. *Chem. Biol.* **1995**, *2*, 409−418.
(31) Elango, N.; Radhakrishnan, R.; Froland, W. A.; Wallar, B. J.; Earhart, C. A.; Lipscomb, J. D.; Ohlendorf, D. H. *Protein Sci.* **1997**, *6*, 556−568.
(32) Lindqvist, Y.; Huang, W.; Schneider, G.; Shanklin, J. *EMBO J.* **1996**, *15*, 4081−4092.
(33) Bollinger, J. M., Jr.; Krebs, C.; Vicol, A.; Chen, S.; Ley, B. A.; Edmondson, D. E.; Huynh, B. H. *J. Am. Chem. Soc.* **1998**, *120*, 1094−1095.

the observed structural changes can help focus ongoing theoretical investigations aimed at defining the structures and reaction pathways of intermediates in O_2 activation at carboxylate-bridged diiron clusters.

Experimental Section

Protein Purification. R2-D84E was isolated as previously described[22,34] and subjected to the following additional purification steps prior to crystallization. The protein (~50 mg) was first loaded on a Mono Q HR 10/10 column (Pharmacia) equilibrated in buffer A (50 mM Tris, 5% glycerol, pH 7.6). After washing the column with 15 mL of buffer A and a 15-mL gradient of 0−15% buffer B (50 mM Tris, 5% glycerol, 1 M NaCl, pH 7.6), the protein was eluted with a 100-mL gradient of 15−45% buffer B. Fractions (3 mL) that contained protein as determined by absorbance at 280 nm were pooled and concentrated to approximately 0.5 mL by using a CentriPrep 30 ultrafiltration device (Amicon). The concentrated sample was then further purified on a Superose 12 HR 10/30 gel filtration column (Pharmacia) equilibrated with 100 mM HEPES, pH 7.6 (flow rate 0.4 mL/min). A final desalting step was performed with an HR 10/10 Fast Desalting Column (Pharmacia) equilibrated with 100 mM HEPES, pH 7.6 (flow rate 1.0 mL/min). The purified R2-D84E sample was then concentrated to 45 mg/mL and flash frozen in liquid nitrogen.

Crystallization. Purified R2-D84E was diluted to 10 mg/mL with 100 mM HEPES, pH 7.6, containing 1 mM EMTS, which was necessary for crystallization,[35] and reconstituted with 6 equiv of Fe^{2+} per dimer, which was added from a stock solution of $Fe(NH_4)_2(SO_4)_2 \cdot 6H_2O$ in 5 mN H_2SO_4. Crystallization was carried out at 37 °C by using the hanging drop method. Drops containing 5 μL of protein solution were added to 5 μL of precipitant solution suspended on the lid of a sealed Petri dish containing 5 mL of precipitant solution. The precipitant solution contained 50 mM MES, pH 6.0, 200 mM NaCl, 20% PEG 4000, 0.3% dioxane, and 1 mM EMTS.[35] After one week of equilibration, the pH of the hanging drops was measured to be 7.0. Crystals appeared in 3−7 days. Large crystals to be used for data collection (0.15 mm × 0.2 mm × 0.5 mm) were soaked for 3−5 min in a cryosolvent composed of precipitant solution with an additional 20% glycerol, mounted in rayon loops, and immediately frozen in liquid nitrogen. The crystals belong to the space group $P2_12_12_1$ with unit cell dimensions $a = 74.1$ Å, $b = 84.6$ Å, and $c = 114.7$ Å.

Chemical Reduction. Chemical reduction was performed at room temperature by soaking the oxidized crystals in a solution of thoroughly degassed precipitant solution supplemented with 3% sodium dithionite and 1 mM phenosafranin, final pH of 5.0. Crystals were transferred to 40-μL hanging drops of this reducing solution suspended over 1-mL reservoirs of 30% sodium dithionite and incubated for 90 min. The crystals were then transferred to a degassed cryosolvent composed of precipitant solution with 20% glycerol and 3% sodium dithionite, mounted in rayon loops, and frozen in liquid nitrogen.

To verify that this chemical reduction procedure converts oxidized R2-D84E to the O_2-reactive diiron(II) form of the protein, the following control experiment was performed. Oxidized, radical-containing R2-D84E was prepared by addition of 3.3 equiv of Fe^{2+} (from a solution of $Fe(NH_4)_2(SO_4)_2 \cdot 6H_2O$ in 5 mN H_2SO_4) to an air-saturated solution of 0.59 mM apo protein. After repeated mixing to ensure sufficient oxygenation, the tyrosyl radical content (0.89 equiv relative to R2-D84E dimer) was determined spectrophotometrically from the dropline-corrected absorbance at 409 nm, $A_{409} - (A_{403} + A_{415})/2$. The direct proportionality of $A_{409} - (A_{403} + A_{415})/2$ to tyrosyl radical concentration had previously been verified. The value of the proportionality constant ($\epsilon_{409} - (\epsilon_{403} + \epsilon_{415})/2$) was determined ($2.17 \times 10^3$ $M^{-1}cm^{-1}$) by comparison of the two quantities for a series of 17 samples. For each sample, the concentration of radical was determined directly by EPR spectroscopy (by comparison of integrated signal intensities to that of a copper-perchlorate standard).[36] To mimic the procedure used for the crystals, chemical reduction of the radical and diiron(III) center was performed by anaerobic addition of dithionite and phenosafranin to final concentrations of 4.91 mM and 1 mM, respectively. After incubation for approximately 5 min, the protein was recovered by anaerobic desalting on a G-25 spin column equilibrated with 100 mM HEPES buffer, pH 7.6, and its absorption spectrum was measured in a septum-sealed cuvette. The recovered protein was then exposed to air for several minutes, and the absorption spectrum measured again.

Table 1. Data Collection and Refinement Statistics

	Ferric R2-D84E	Ferrous R2-D84E
	data collection	
wavelength (Å)	1.08	1.0045
resolution range (Å)	35−2.2	35−1.98
unique reflcns	39389	49651
total observations	364520	480461
completeness (%)[a]	99.4 (99.8)	98.7 (98.8)
R_{sym}[b]	0.068 (0.248)	0.074 (0.298)
	refinement	
resolution range (Å)	25−2.2	25−1.98
no. of reflns	36848	47987
R factor[c]	0.190	0.205
R free	0.232	0.245
no. of protein atoms	5572	5572
rms bond length (Å)	0.007	0.007
rms bond angles (deg)	1.1	1.1
av *B*-value (Å^2)		
main chain	23.5	26.9
side chain	26.8	32.0

[a] Values in parentheses are for the highest resolution shells. [b] $R_{sym} = \sum|I_{obs} - I_{avg}|/\sum I_{obs}$, where the summation is over all reflections. [c] *R*-factor $= \sum|F_{obs} - F_{calc}|/\sum F_{obs}$. Five percent of the reflections were reserved for calculation of *R*-free.

Data Collection and Refinement. Diffraction data for oxidized R2-D84E were collected at −160 °C at Stanford Synchrotron Radiation Laboratory (SSRL) using a Mar 300 imaging plate detector. Diffraction data for reduced R2-D84E were collected at −160 °C at the Dupont-Northwestern-Dow Collaborative Access Team (DND-CAT) beamline at the Advanced Photon Source using a 2k × 2k Mar CCD detector. All data were processed with the programs DENZO and SCALEPACK (Table 1).[37] Both structures were refined with X-PLOR[38] and CNS[39] using the refined coordinates of oxidized wt R2[40] without solvent molecules as a starting model. After rigid body refinement at 3.0 Å resolution, iterative cycles of simulated annealing, individual *B*-factor refinement, and model rebuilding with the program O[41] were performed. Upon lowering the occupancy of any of the four iron sites below 100%, positive peaks in $F_o - F_c$ electron density maps were apparent, suggesting that all four iron sites are fully occupied. Solvent molecules modeled at peaks $>3\sigma$ in $F_o - F_c$ maps were retained if the *B*-values refined to <60 Å^2. The progress of the refinement was monitored by the *R*-free, which was calculated using 5% of the data (Table 1). A Ramachandran plot calculated with PROCHECK[42] indicates that 93.3% of the residues in the oxidized structure fall in the most favored regions, with 6.2% in the additionally allowed regions. For the chemically reduced structure, 92.8% of the residues fall in the most favored regions, with 6.8% in the additionally allowed regions. The average error in coordinate positions was estimated by a Luzzati plot to be 0.22 Å for

(34) Parkin, S. E.; Chen, S.; Ley, B. A.; Mangravite, L.; Edmondson, D. E.; Huynh, B. H.; Bollinger, J. M., Jr. *Biochemistry* **1998**, *37*, 1124−1130.

(35) Nordlund, P.; Uhlin, U.; Westergren, C.; Joelson, T.; Sjöberg, B.-M.; Eklund, H. *FEBS Lett.* **1989**, *258*, 251−254.

(36) Vicol, A.; Ley, B. A.; Bollinger, J. M., Jr. Unpublished results.

(37) Otwinowski, Z.; Minor, W. *Methods Enzymol.* **1997**, *276*, 307−326.

(38) Brünger, A. T. *X-PLOR Version 3.1 Manual: A system for X-ray crystallography and NMR*; Yale University Press: New Haven, CT, 1993.

(39) Brünger, A. T.; Adams, P. D.; Clore, G. M.; DeLano, W. L.; Gros, P.; Grosse-Kunstleve, R. W.; Jiang, J.-S.; Kuszewski, J.; Nilges, M.; Pannu, N. S.; Read, R. J.; Rice, L. M.; Simonson, T.; Warren, G. L. *Acta Crystallogr.* **1998**, *D54*, 905−921.

(40) Nordlund, P.; Eklund, H. *J. Mol. Biol.* **1993**, *231*, 123−164.

(41) Jones, T. A.; Zou, J.-Y.; Cowan, S. W.; Kjeldgaard, M. *Acta Crystallogr.* **1991**, *A47*, 110−119.

(42) Laskowski, R. A. *J. Appl. Crystallogr.* **1993**, *26*, 283−291.

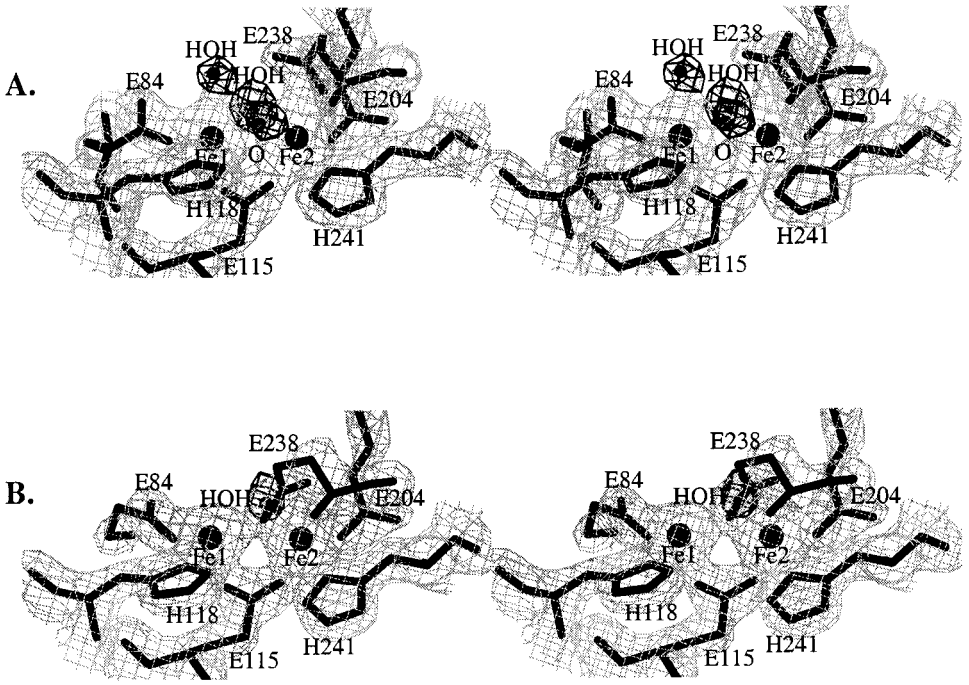

Figure 1. (A) Stereoview of the final 2.2 Å resolution $2F_o - F_c$ electron density map at the diiron site in oxidized R2-D84E (gray, contoured at 1.4σ). The $F_o - F_c$ map showing the coordinated water molecules is superimposed (black, contoured at 4.5σ). (B) Stereoview of the final 1.98 Å resolution $2F_o - F_c$ electron density map at the diiron site in reduced R2-D84E (gray, contoured at 1.4σ). The $F_o - F_c$ map showing the coordinated water molecules is superimposed (black, contoured at 3σ).

both structures. The final electron density maps at the active sites are shown in Figure 1. Figure 1 was generated with BOBSCRIPT,[43] and Figures 2 and 3 were generated with MOLSCRIPT.[44]

Results

Structure of Oxidized R2-D84E. The diiron(III) center in oxidized R2-D84E (Figures 1A and 2A) closely resembles that in wt R2[40] with similar coordination and an average Fe···Fe distance of 3.36 Å (Table 2). Two differences are notable, however. First, the structures differ in the coordination mode of residue 84. In wt R2, D84 is bidentate chelating to Fe1 whereas in R2-D84E, E84 coordinates to Fe1 in a monodentate, terminal mode. The uncoordinated oxygen atom of E84 is hydrogen bonded to a coordinated water molecule. Second, the average Fe1−Y122OH distance of 6.22 Å (Table 2) is longer than the 5.3 Å distance observed in wt R2.[40] In wt R2, the side chain oxygen atoms of D84 and Y122 are close enough to form a hydrogen bond, but the shifted position of Y122 in R2-D84E prevents a similar interaction between E84 and Y122.

Structure of Reduced R2-D84E. After chemical reduction, the diiron center structure shown in Figures 1B, 2C, and 3 was obtained. To establish that the chemical reduction procedure used for the crystals converts oxidized R2-D84E to the O_2-reactive diiron(II) form of the protein, a solution of R2-D84E containing 0.89 equiv of tyrosyl radical was reduced by the same method. After anaerobic removal of the dithionite and phenosafranin, the spectrum of this sample exhibited only very weak absorption at 320 and 365 nm from the μ-oxodiiron(III) cluster and indicated that only 0.04 equiv of tyrosyl radical remained. We attribute both of these features to contamination with trace O_2 during or after chromatographic removal of the dithionite/phenosafranin. Exposure of this sample to oxygen by removal of the septum from the cuvette and repeated mixing led to regeneration of 0.79 equiv of tyrosyl radical and reappearance of the 320- and 365-nm features of the μ-oxodiiron(III) cluster. These results demonstrate that, at least for the protein in solution, the chemical reduction procedure does indeed reduce the diiron(III) cluster to the O_2-reactive diiron(II) state. On the basis of this result and the structural adjustments observed following application of the chemical reduction procedure to the crystal (vide infra), we conclude that the species obtained after this procedure is the diiron(II) form of the protein.

Comparison of the diiron(II) center in R2-D84E (Figures 1B, 2C, and 3) to that in wt R2[28] (Figures 2B and 3) reveals three significant differences involving carboxylate ligands. First, E84 is bidentate chelating to Fe1 whereas in the reduced wt R2 structure, D84 was assigned as a monodentate, terminal ligand. Second, the conformation of E204 has changed considerably. In wt R2, E204 adopts a syn monodentate, terminal coordination mode in one monomer and is chelating in the other monomer. In R2-D84E, E204 adopts an anti monodentate, terminal coordination mode in both monomers. The uncoordinated oxygen atom of this residue is clearly hydrogen bonded to a water molecule in monomer B, and weak electron density is present in monomer A at the position of this water molecule. Third, the coordination mode of E238 is altered. The two Fe ions are bridged by E238 in a μ-(1,3) fashion in the wt R2 structure. In R2-D84E, E238 adopts a μ-(η^1,η^2) coordination mode, with just one oxygen atom bridging the two Fe ions and Fe2 coordinated by both oxygen atoms. As a result, the average Fe···Fe distance is reduced from 3.9 Å in wt R2 to 3.5 Å in R2-D84E (Table 3). This type of coordination was also observed for E238 in the azide adduct of the F208A/Y122F double mutant of R2.[17] There is one solvent molecule coordinated to Fe2, located in the same position occupied by azide in the F208A/Y122F azide adduct structure. Thus, Fe1 is five-coordinate and Fe2 is six-coordinate. By contrast, both Fe ions are four-coordinate in reduced wt R2, and no exogenous ligands are present. As observed for the oxidized form, the average Fe1−Y122OH distance in reduced R2-D84E is ∼1 Å longer than

(43) Esnouf, R. M. *J. Mol. Graphics Model.* **1997**, *15*, 132−134.
(44) Kraulis, P. J. *J. Appl. Crystallogr.* **1991**, *24*, 946−950.

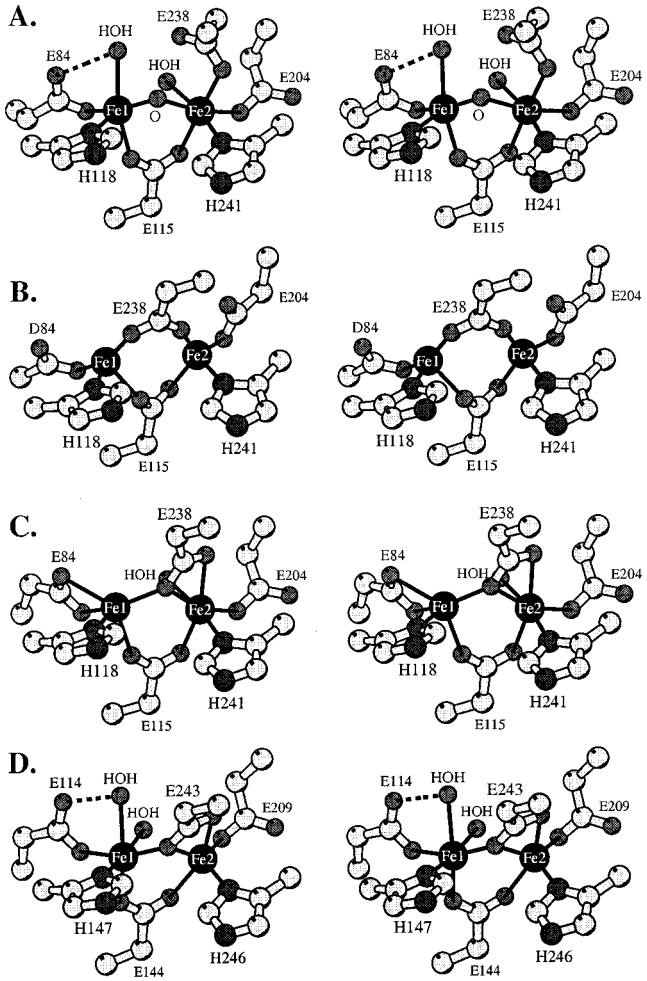

Figure 2. (A) Stereoview of the diiron center in oxidized R2-D84E. The two independent diiron centers in the halves of the R2 dimer have the same coordination geometry. (B) Stereoview of the diiron center in reduced wt R2.[28] (C) Stereoview of the diiron center in chemically reduced R2-D84E. The two independent diiron centers in the halves of the R2 dimer have the same coordination geometry. (D) Stereoview of the diiron center in reduced MMOH.[30]

that in reduced wt R2 (Table 3, Figure 3). Consequently, a hydrogen bond linking the uncoordinated oxygen atom of D84 and the phenolic hydroxy group of Y122 in reduced wt R2[28] is not present in reduced R2-D84E.

Comparison of Reduced R2-D84E with Reduced MMOH. The diiron(II) cluster in R2-D84E is quite similar to that in the chemically reduced, diiron(II) form of MMOH (Figure 2D).[30] The μ-(η^1,η^2) conformation of E238 is nearly identical with that of the corresponding residue, E243, in MMOH. The conformation of E204 is very similar to the conformation of its MMOH counterpart, E209, and the uncoordinated oxygen atom of MMOH E209 is also hydrogen bonded to a water molecule.[45] Finally, the 3.5 Å Fe···Fe distance in R2-D84E is closer to the 3.3 Å Fe···Fe distance in MMOH[30] than to the 3.9 Å distance in reduced wt R2.[28] These similarities are especially striking when considered with the observations that MMOH[5,7] and R2-D84E[22,33] accumulate peroxo intermediates with nearly identical spectroscopic signatures while wt R2 fails to accumulate this species.[23] The two structures differ in the positions of coordinated solvent molecules. In MMOH, two water molecules are coordinated to Fe1, one forming a hydrogen bond to E114.[30] In reduced R2-D84E, no exogenous ligands are bound to Fe1, and one water molecule is coordinated to Fe2.

(45) Dunietz, B. D.; Beachy, M. D.; Cao, Y.; Whittington, D. A.; Lippard, S. J.; Friesner, R. A. *J. Am. Chem. Soc.* In press.

Discussion

Our ultimate goal in carrying out structural and mechanistic characterization of wt R2 and its engineered variants is to define, in terms of the atomic and electronic motions that can occur during O_2 activation at a carboxylate-bridged diiron cluster, the precise mechanisms by which the reactivity of the cluster can be modulated by its protein chelator. In the present study we sought to address how a substitution that amounts to addition of a methylene linker to a carboxylate ligand (D84) to one Fe ion of the cluster either *stabilizes the μ-1,2-peroxodiiron(III) complex* by at least 400-fold (in a kinetic sense) relative to the same adduct in the wt protein or *causes the μ-1,2-peroxodiiron-(III) complex to form* in preference to a more reactive, structurally distinct adduct that forms in the wt protein. Although the structure of reduced R2-D84E shows that the seemingly minor alteration propogates changes through the cluster that render it more similar to that in MMOH, both technical considerations and gaps in current mechanistic understanding preclude assignment of a specific cause for accumulation of the intermediate in the variant protein.

First, the flexibility in coordination revealed by the differences between the reduced and oxidized forms of MMOH,[30] wt R2,[28] and R2-D84E suggests that structural isomers of a given cluster might have similar energies. In no case has it been established that the form of the cluster present in the chemically reduced crystal reacts efficiently with O_2. For MMOH, this is likely *not* to be the case, since component B, which was not present in the crystal, is required in solution for proper O_2 reactivity and is known to induce a structural change at the cluster upon binding to MMOH.[46] For different reasons, a similar caveat must be attached to the wt R2 and R2-D84E structures. In these studies, the pH of the mother liquor bathing the crystal was between 5 and 6 after the chemical reduction procedure, whereas oxygen activation by each protein has been studied primarily at pH 7.6. An effect of pH on cluster coordination in reduced wt R2 might explain why the geometry seen in the crystallographic studies (two four-coordinate Fe(II) ions) does not completely agree with that deduced from CD/MCD spectroscopy of samples at pH 7.6 (one 5-coordinate and one 4-coordinate Fe(II) ion).[47] Similarly, preliminary CD/MCD studies on diferrous R2-D84E (at pH 7.6) also suggest differences from the coordination geometry observed in our crystallographic study.[48] Clearly, additional studies are required to establish whether the published structures accurately represent the O_2-reactive cluster forms.

Second, because the identities of precursors to **X** in wt R2 have not been established, it is unclear whether the reduced R2-D84E structure should be used to explain a simple decrease in reactivity of the μ-1,2-peroxodiiron(III) complex in R2-D84E or a change in the mechanistic pathway. Even if we invoke the apparently popular presumption that the wt R2 and R2-D84E mechanisms differ only in rate constants of constitutent steps, insight into the pathway(s) for breakdown of the μ-1,2-peroxodiiron(III) complex in wt R2 is required to determine which step is retarded by the structural adjustments accompanying the D84E substitution. Such detailed mechanistic under-

(46) Pulver, S. C.; Froland, W. A.; Lipscomb, J. D.; Solomon, E. I. *J. Am. Chem. Soc.* **1997**, *119*, 387−395.

(47) Pulver, S. C.; Tong, W. H.; Bollinger, J. M., Jr.; Stubbe, J.; Solomon, E. I. *J. Am. Chem. Soc.* **1995**, *117*, 12664−12678.

(48) Yang, Y.-S.; Baldwin, J.; Ley, B. A.; Bollinger, J. M., Jr.; Solomon, E. I. Unpublished results.

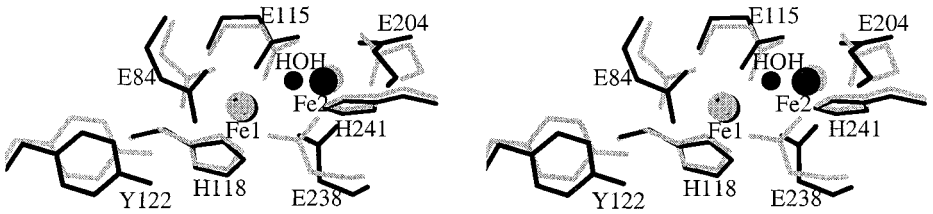

Figure 3. Stereo superposition of the active sites in reduced R2-D84E (black) and in reduced wt R2 (gray). The shifts in residues E84, E204, E238, and Y122 are apparent.

Table 2. Interatomic Distances (Å) in Diferric R2-D84E

atom	atom	monomer A	monomer B	av
Fe1	Fe2	3.33	3.38	3.36
Fe1	Glu84 Oϵ1	2.18	2.09	2.14
	Glu84 Oϵ2	2.93	2.69	2.81
	Glu115 Oϵ1	2.11	2.15	2.13
	His118 Nδ1	2.41	2.40	2.40
	μO	1.94	2.16	2.05
	OH_2	2.49	2.46	2.48
	Tyr 122 OH	6.04	6.40	6.22
Fe2	Glu115 Oϵ2	2.21	2.15	2.18
	Glu204 Oϵ1	2.16	2.18	2.17
	Glu238 Oϵ1	2.06	2.13	2.10
	His241 Nδ1	2.17	2.23	2.20
	μO	2.24	2.17	2.20
	OH_2	2.26	2.38	2.32
Glu84 Oϵ2	OH_2 (Fe1)	3.00	2.61	2.80
Glu238 Oϵ2	OH_2 (Fe1)	2.71	2.93	2.82
	OH_2 (Fe2)	2.56	2.81	2.68

Table 3. Interatomic Distances (Å) in Diferrous R2-D84E

atom	atom	monomer A	monomer B	av
Fe1	Fe2	3.44	3.53	3.48
Fe1	Glu84 Oϵ1	2.27	2.33	2.30
	Glu84 Oϵ2	2.55	2.39	2.47
	Glu115 Oϵ1	2.17	2.18	2.18
	His118 Nδ1	2.26	2.27	2.26
	Glu238 Oϵ1	2.45	2.41	2.43
	OH_2	2.98	2.89	2.94
	Tyr 122 OH	5.91	6.49	6.20
Fe2	Glu115 Oϵ2	2.27	2.10	2.18
	Glu204 Oϵ1	2.24	2.30	2.27
	Glu238 Oϵ1	2.32	2.31	2.32
	Glu238 Oϵ2	2.34	2.23	2.28
	His241 Nδ1	2.26	2.25	2.26
	OH_2	2.21	2.45	2.33

standing is lacking, even for the MMOH reaction, in which the intermediacy of the peroxo complex is more well-established. Thus, more complete characterization of both the R2-D84E and the wt R2 reactions is also required if a cause for accumulation of the peroxo complex in the former but not the latter is to be extracted from the structural data.

Despite these current limitations, the structures of reduced and oxidized R2-D84E represent a key intial step in our approach to understanding protein control of diiron cluster reactivity. Our aim is to develop a "training set" of crystallographically characterized, closely related variant proteins with defined and different reactivities to identify functionally significant variations among the many that occur in the natural proteins. Although structures have been determined for only two of the variants for which mechanistic data are available (wt and D84E), these structures can help calibrate computational studies aimed at defining the detailed mechanistic pathway(s) for O_2 activation at diiron(II) clusters. The R2-D84E structures are particularly relevant to the conclusions of three such studies.

Structures having μ-(η^1,η^2) peroxide coordination have recently been proposed as candidates for MMOH **P** in two separate studies by Siegbahn et al.[49] and Dunietz et al.[45] A unique conclusion of the latter study is that the stability of this structure depends on a network of hydrogen bonds connecting the uncoordinated oxygen of E114 (the residue corresponding to D84 in R2), a water molecule coordinated by Fe1, and the singly coordinated peroxide oxygen. These authors proposed that a similar network might stabilize the peroxide complex in R2-D84E. Although the postulated Fe1-coordinated water molecule is not present in the structure of reduced R2-D84E, it is present in the oxidized protein and is hydrogen bonded to the uncoordinated oxygen atom of E84, as was proposed for the peroxo intermediate. A possible reaction scheme for conversion of the R2-D84E diiron(II) cluster to the diiron(III) cluster through a peroxo intermediate might involve (1) replacement at Fe1 of the oxygen atom of E84 that is trans to E115 by a water molecule with loss of the Fe2-coordinated water, (2) subsequent or concomitant formation of the peroxide intermediate, and (3) cleavage of the peroxide so that one oxygen atom ends up as the oxo bridge and the other as the *Fe2*-coordinated water of the product. This scheme would permit formation of a peroxo intermediate of precisely the structure proposed by Dunietz et al., and could also provide a structural rationale for accumulation of the peroxo complex in R2-D84E but not wt R2 on the basis of a lower ground-state energy of the complex in the variant protein. In support of this idea, the D84E substitution induces a tilt of the carboxylate of residue 84, which moves the key oxygen atom toward the position occupied by the Fe1-coordinated water molecule in the diiron(III) cluster. In addition, the substitution fractures a potentially competing hydrogen bond that is present in reduced wt R2 between the uncoordinated oxygen atom of D84 and the phenolic hydroxyl group of Y122.

Although stabilization of the R2-D84E peroxo intermediate by hydrogen bonding is consistent with available experimental data, the question of what mechanistic pathway the reaction of the wt protein might take in the absence of the optimized hydrogen bonding network remains unresolved. In the simplest scenario, a similar peroxo complex would form, but would have a higher ground-state energy and decay more rapidly. It is also possible that a superoxo intermediate with a formal cluster oxidation state of Fe(II),Fe(III) might be the precursor to **X** in wt R2, perhaps accepting the extra electron itself instead of isomerizing to the peroxo complex. In this scenario, a complex with a terminal peroxide ligand and a formal Fe(II), Fe(III) cluster oxidation state would form, and could rearrange rapidly to **X** in a process involving O−O bond cleavage. This possibility is underscored by the suggestion made by both Siegbahn et al.[49] and Dunietz et al.[45] that formation of **P** in MMOH might proceed stepwise through such a species. The D84E substitution might simply modulate the relative rates of direct reduction of this hypothetical **X** precursor versus isomerization to the more stable peroxo complex. In wt R2, the former process might

(49) Siegbahn, P. E. M.; Crabtree, R. H. *J. Am. Chem. Soc.* **1997**, *119*, 3103−3113.

successfully compete, whereas in the D84E variant, the latter would predominate as a consequence of either a decrease in the rate of reduction or (more likely) an increase in the rate of isomerization to the peroxo complex (which might be related to the aforementioned optimization of the hydrogen bond network involving E84). Alternatively, a superoxo complex need not even be on the pathway to the peroxo complex in R2-D84E. The adjustments in coordination associated with the D84E substitution might be sufficient to direct formation of the peroxo complex in preference to a rapidly reacting superoxo complex favored in the wt protein. One possible geometry for such a species would have the superoxide coordinated only to Fe1 in an η^2-mode. Such a structure would be favored by, or might even require, a four-coordinate Fe(II) ion at this site. The altered coordination mode of residue 84 results in a five-coordinate Fe(II) ion and might therefore disfavor O_2 access to the coordination site appropriate to form the rapidly reacting species.

Whereas the hypotheses of Dunietz et al. implicate ground-state stabilization of the peroxo complex by the D84E substitution, an earlier spectroscopic and computational study of a μ-1,2-peroxodiiron(III) model complex by Brunold et al.[50] suggests a possible mechanism by which the energy of the transition state for decay might be increased as a result of the substitution. These authors proposed that decay of the complex to a **Q**-like diiron(IV) species could be initiated by protonation of the peroxide and a shift to a μ-1,1 bridging mode. This possibility is consistent with the recent report that a proton is taken up during the conversion of **P** to **Q** in MMOH from *M. trichosporium* O3B.[51] It is possible that one of the R2 residues which undergoes adjustment as a result of the D84E substitution participates in protonation of the peroxide. A candidate for the proton donor is Y122, since spectroscopic data have established that the radical formed upon oxidation of this residue is neutral (unprotonated).[52,53] The hydrogen bond between Y122 and the uncoordinated oxygen of D84 in the reduced wt protein might position Y122 for efficient proton transfer to the peroxide, which could be mediated by the D84 carboxylate or an Fe1-coordinated water molecule or both. As previously pointed out by Burdi et al.,[54] this step would have the additional effect of priming Y122 for oxidation from the more reactive phenolate form. If this were the case, the altered position of the carboxylate of E84 and the accompanying loss of the hydrogen bond to Y122 would retard decay of the peroxo complex by disfavoring its protonation. However, substitution of the Y122 side chain with an aprotic one would also be expected to slow decay of the peroxo complex, and no evidence for accumulation of the complex in the extensively studied Y122F variant has been reported. Alternatively, a coordinated water molecule might provide the proton itself without re-acquiring one from Y122 via D84. Because no coordinated water molecule is observed in reduced wt R2 and the positions of the two coordinated water molecules in oxidized wt R2 are nearly identical with those in oxidized R2-D84E, it is not easy to envisage how the structural adjustments in the variant protein might impede proton transfer to the peroxide from a water ligand.

Clearly, there are multiple potential explanations for the effect of the D84E substitution, of which we have discussed only a few. Given the myriad possibilities, it would be of immense value in identifying the *actual* cause to have a structure of the peroxo complex itself. Although there are several technical obstacles that still must be overcome to achieve this goal, the present structure and our studies of the R2-W48F/D84E variant, in which the peroxo complex is even more stable, set the stage for such structural characterization.

Acknowledgment. This work was supported by funds from the Robert H. Lurie Cancer Center at Northwestern University (A.C.R.), by NIH grant GM55365 (J.M.B.), and by grants from the Searle Scholars Program of the Chicago Community Trust and the Camille and Henry Dreyfus Foundation (J.M.B). Stanford Synchrotron Radiation Laboratory (SSRL) is funded by the Department of Energy, Office of Basic Energy Sciences, and the DND-CAT Synchrotron Research Center at the Advanced Photon Source is supported by E.I. DuPont de Nemours & Co., The Dow Chemical Company, the NSF, and the State of Illinois. We thank S. J. Lippard for providing a preprint of ref 45.

JA991839L

(50) Brunold, T. C.; Tamura, N.; Kitajima, N.; Moro-oka, Y.; Solomon, E. I. *J. Am. Chem. Soc.* **1998**, *120*, 3074−3090.

(51) Lee, S.-K.; Lipscomb, J. D. *Biochemistry* **1999**, *38*, 4423−4432.

(52) Bender, C. J.; Sahlin, M.; Babcock, G. T.; Barry, B. A.; Chandrashekar, T. K.; Salowe, S. P.; Stubbe, J.; Lindström, B.; Petersson, L.; Ehrenberg, A.; Sjöberg, B.-M. *J. Am. Chem. Soc.* **1989**, *111*, 8076−8083.

(53) Backes, G.; Sahlin, M.; Sjöberg, B.-M.; Loehr, T. M.; Sanders-Loehr, J. *Biochemistry* **1989**, *28*, 1923−1929.

(54) Burdi, D.; Willems, J.-P.; Riggs-Gelasco, P.; Antholine, W. E.; Stubbe, J.; Hoffman, B. M. *J. Am. Chem. Soc.* **1998**, *120*, 12910−12919.